INTERNATIONAL JOURNAL FOR NUMERICAL METHODS IN ENGINEERING, VOL. 20, 1111-1129 (1984)

THE POST-PROCESSING APPROACH IN THE FINITE ELEMENT METHOD—PART 2: THE CALCULATION OF STRESS INTENSITY FACTORS†

I. BABUŠKA AND A. MILLER
Institute for Physical Science and Technology, University of Maryland, College Park, Maryland, U.S.A.

SUMMARY

In the context of a model problem we describe post-processing techniques for the calculation of generalized stress intensity factors as well as displacements, stresses, etc., near corner points. We discuss two broad classes of methods, one involving an 'influence' function, and the other related to the well-known energy release principle of fracture mechanics. An error analysis is sketched and two numerical examples are given to illustrate the effectiveness of the techniques.

1 INTRODUCTION

1.1 *General introduction*

This is the second in a series of three papers in which we discuss post-processing as it may be applied in the finite element method. In the first paper[1] we briefly described some general aspects of post-processing, and illustrated a few of the ideas in the particular cases of some model problems from structural mechanics and seepage analysis. For these model problems we were concerned with obtaining values for the displacement, stresses, bending moment, flow rate, etc., either at a point or as an average over some subsection of a region. However, we were careful to note that for two-dimensional problems the methods discussed could only be expected to perform well if the point of subsection under consideration was 'reasonably distant' from certain critical points (e.g. corner points) of the region. In this paper we take up the problem of how to proceed when this 'reasonably distant' criterion is no longer satisfied.

As is well known, corner points or points where the nature of boundary conditions change usually give rise to some form of singular behaviour in the solutions of many important problems. In fact, the stress intensity factors of elasticity theory are the coefficients of the terms that exhibit this singular behaviour. They serve as a means of characterizing the state of stress in the neighbourhood of the critical point. We shall see that calculation of these stress intensity factors, as well as certain coefficients of non-singular terms, is possible within a post-processing scheme. The values of displacements or stresses at points near the critical point may then be found by using the values of the stress intensity factors, along with the non-singular coefficients, in known asymptotic expansions valid in the vicinity of the critical point.

For the seepage analysis problem of Section 4 of Reference 1 there are obvious analogues of the stress intensity factors of elasticity. They are the coefficients of the singular terms in the

† This research was partially supported by ONR Contract N00014-77-C-0623. The computations were carried out with support from the Computer Science Center of the University of Maryland, College Park, MD, U.S.A.

0029-5981/84/061111-19$01.90

Received 20 December 1982
Revised 21 April 1983

asymptotic expansion of the flow velocity near such critical points as the tip of the grout curtain or the downstream edge of the base of the dam. Post-processed values for such coefficients may be substituted into asymptotic expansions of known form to yield pointwise values for the flow velocity.

In this paper the post-processing calculations will be based on extraction expressions that are of the general form

$$\Phi = \Phi(\omega) = \int_\Omega \lambda \,.\, \nabla\omega \, dA + \int_\Omega \zeta\omega \, dA + \int_{\partial\Omega} \rho\omega \, ds + R \tag{1}$$

where $\lambda = (\lambda_1, \lambda_2)$ is a vector function on Ω, ζ is a scalar function on Ω, ρ is a scalar function defined on the boundary $\partial\Omega$ of Ω, or some specified portion of $\partial\Omega$, and R is an integral which is easily computable from the load data of the problem. In conformity with the terminology of Subsection 1.1 of Reference 1, we shall refer to λ, ζ and ρ as extraction functions, and R will be called the load term. If $\tilde{\omega}$ is a finite element approximation to ω, then (1) suggests that we use

$$\tilde{\Phi} = \tilde{\Phi}(\tilde{\omega}) = \int_\Omega \lambda \,.\, \nabla\tilde{\omega} \, dA + \int_\Omega \zeta\tilde{\omega} \, dA + \int_{\partial\Omega} \rho\tilde{\omega} \, ds + R \tag{2}$$

as an approximation to Φ (cf. (2) of Reference 1).

1.2 Formulation of the model problem

For the most part our discussion in this paper will be in the setting of a particular model problem. Suppose Ω is a bounded, two-dimensional region whose boundary is made up of smooth arcs $\Gamma_1, \ldots, \Gamma_s$. Consider a boundary value problem governed by the equation

$$\nabla^2\omega = -p \quad \text{in } \Omega \tag{3a}$$

and for which, independently on each Γ_j, either the Dirichlet boundary condition

$$\omega = f_j \quad \text{on } \Gamma_j \tag{3b}$$

or the Neumann boundary condition

$$(\nabla\omega) \,.\, \hat{n} = g_j \quad \text{on } \Gamma_j \ (\hat{n} = \text{outward pointing unit normal}) \tag{3c}$$

applies. For definiteness, assume that Γ_1 and Γ_2 are adjacent edges of Ω which meet at the origin of the co-ordinate system (x_1, x_2). Establish polar co-ordinates (r, θ) at this origin, and suppose that Γ_1 and Γ_2 are in fact straight-line segments which correspond to $\theta = 0$ and $\theta = \alpha\pi$, respectively. Assume that in the vicinity of O the region Ω corresponds to the cone $0 < \theta < \alpha\pi$ (see Figure 1). For Γ_1 and Γ_2, let the boundary conditions (3b) and (3c) take the specific form

$$\omega = f_1 = 0 \quad \text{on } \Gamma_1 \qquad \text{and} \qquad (\nabla\omega) \,.\, \hat{n} = g_2 = 0 \quad \text{on } \Gamma_2 \tag{3d}$$

(If $\alpha = 2$, then what we have described models a slit membrane. The upper face ($\theta = 0$) of the slit is fixed, whereas the lower face ($\theta = 2\pi$) has no line load.)

In a neighbourhood of the vertex O the solution ω and its derivatives have asymptotic expansions of the form

$$\omega = \sum_{n=1}^{N} k_n r^{(2n-1)(1/2\alpha)} \sin\left((2n-1)\frac{\theta}{2\alpha}\right) + \sigma(r^{(2N-1)(1/2\alpha)}) \tag{4a}$$

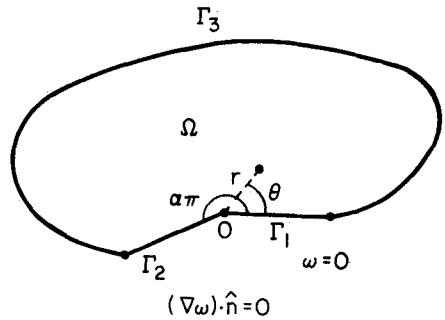

Figure 1. Region for model problem (3)

$$\nabla\omega = \sum_{n=1}^{N} \frac{2n-1}{2\alpha} k_n r^{(2n-1-2\alpha)(1/2\alpha)} \begin{pmatrix} \sin\left((2n-1-2\alpha)\dfrac{\theta}{2\alpha}\right) \\ \cos\left((2n\cdot\cdot 1-2\alpha)\dfrac{\theta}{2\alpha}\right) \end{pmatrix} + o(r^{(2N-1-2\alpha)(1/2\alpha)}) \quad (4b)$$

for some numbers k_n, $n = 1, \ldots, N$. If the body fo.ce p vanishes in a neighbourhood of O, then the integer N is arbitrary. More generally, the values of N for which the above expansions are valid depend on the local smoothness of p. If $p \in L_2(\Omega)$, i.e. p is a square integrable function, then (4a) and (4b) hold provided $N < \alpha + \frac{1}{2}$ (see Reference 2). Provided p, the f_j and g_j's are sufficiently smooth, then in the vicinity of any other vertex, P say, of Ω

$$\begin{aligned} \omega &= O(1) \\ \nabla\omega &= O(|x - x(P)|^{-3/4}) \end{aligned} \quad (5)$$

where $|x-x(P)| = [(x_1 - x_1(P))^2 + (x_2 - x_2(P))^2]^{1/2}$. See Reference 2 for further details. Notice that if $n < \frac{1}{2} + \alpha$, the nth term in the expansion (4b) for $\nabla\omega$ is unbounded as $r \to 0$. We can think of the coefficients k_n of these terms as analogues of the stress intensity factors of elasticity. In this paper we generalize this terminology somewhat, and refer to all the coefficients k_n, whether or not the corresponding terms in (4) are singular, as stress intensity factors.

Our approach to obtaining approximate values for the 'displacement' ω and the 'stress' $\partial\omega/\partial x_j$ near O will be to first calculate the coefficients k_n by a post-processing of the finite element solution, and then use the asymptotic expansions (4) to find the displacement and stresses. Notice that this is a reversal of a 'standard' method which is often used to calculate the stress intensity factors: first, the finite element solution is 'fitted' in some way to (4), and the resulting coefficients corresponding to the k_n are taken as the appropriate stress intensity factors.

Although most of our attention in this paper will be centred on the above model problem, the ideas of our analysis extend in a natural way to many other two-dimensional problems. In particular, if instead of the mixed boundary condition (3d), either a homogeneous Neumann or homogeneous Dirichlet boundary condition is imposed on both Γ_1 and Γ_2, then there would be no essential difference in our analysis. (In these cases, the expansions in (4) will be powers of $r^{1/\alpha}$, not $r^{1/2\alpha}$.) The case of non-homogeneous boundary conditions on Γ_1 and Γ_2 can also be treated. Everything we do could also be carried out in the context of two-dimensional linear elasticity (see Section 5 and Reference 13).

1.3 *Outline of the paper*

In Sections 2 and 3 we derive two different expressions for the stress intensity factors k_n of (4). These expressions are both of the general form described by (2). Section 4 addresses the accuracy of the post-processed approximations to k_n based on these expressions. Our discussion at this point will be very similar to that in the corresponding section of our earlier paper. In Section 5 we briefly describe a number of extraction expressions for the classical mode I and mode II stress intensity factors of linear fracture mechanics. Finally, in Section 6 we give two numerical examples to illustrate the practical effectiveness of post-processing in the context of the model problem (3).

2 THE GENERALIZED INFLUENCE FUNCTION METHOD

2.1

The first method for calculating stress intensity factors that we shall describe is based on an influence function approach. At least in theory, the concept of an influence function for a stress intensity factor has been known for some time (see, for instance, References 3 and 12). However, these kinds of ideas do not appear to be widely used in finite element practice (see, however, References 4, 5 and 10). Although what we shall say will only be in the context of the model problem (3), the ideas may be readily extended to other situations.

2.2 *An expression for k_m*

Let φ be a function defined on Ω. For the moment, let us only assume that φ is smooth everywhere in Ω except, perhaps, near the corner of interest at O. Let P_l $(l=0,\ldots,s-1)$ be some enumeration of the vertices of Ω, with P_0 denoting the vertex O. For $\varepsilon>0$, sufficiently small, remove from Ω discs of radius ε about each P_l. Denote by Ω_ε the new region so formed. Let $\Gamma_j^{(\varepsilon)}$ and $\gamma_l^{(\varepsilon)}$ be as indicated in Figure 2. Multiply (3a) by φ and integrate by parts over Ω_ε to obtain

$$-\int_{\Omega_\varepsilon} p\varphi \, dA = \int_{\Omega_\varepsilon} (\nabla^2\omega)\varphi \, dA = \left(\sum_l \int_{\gamma_l^{(\varepsilon)}} + \sum_j \int_{\Gamma_j^{(\varepsilon)}}\right)(\nabla\omega \cdot \hat{n}\varphi - \nabla\varphi \cdot \hat{n}\omega)\, ds$$

$$+\int_{\Omega_\varepsilon} (\nabla^2\varphi)\omega \, dA, \tag{6}$$

where $\hat{n}$ is the outward pointing unit normal.

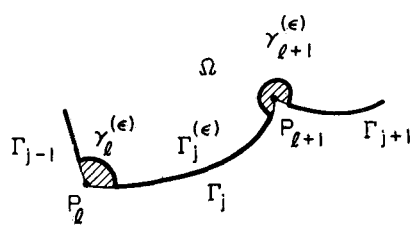

Figure 2. Detail of corner points of Ω

Now, let us place some further restrictions on the generating function φ. Suppose that

1. $\varphi = 0$ on each of the edges Γ_j to which the Dirichlet boundary condition (3b) applies.
2. In the vicinity of the vertex O,

$$\varphi = \frac{2}{\pi(2m-1)} r^{-(2m-1)(1/2\alpha)} \sin\left((2m-1)\frac{\theta}{2\alpha}\right) + \varphi_b$$

for some $m = 1, 2, \ldots$ and some smooth function φ_b (bounded second derivatives will suffice).

Using the above properties of φ, along with the expansions (4) and (5), we may directly evaluate the line integrals over the $\gamma_l^{(\varepsilon)}$'s appearing in (6). This gives

$$\int_{\gamma_l^{(\varepsilon)}} (\nabla\omega \,.\, \hat{n}\varphi - \nabla\varphi \,.\, \hat{n}\omega)\, \mathrm{d}s = \begin{cases} -k_m + o(1) & \text{if } l = 0 \\ o(1) & \text{if } l \neq 0 \end{cases}$$

Taking the limit as $\varepsilon \to 0$ in (6), and recognizing that $\nabla^2\varphi$ is bounded near O, leads to the following expression for k_m:

$$k_m = \int_\Omega (\nabla^2\varphi)\omega \, \mathrm{d}A + \sum_j^N \int_{\Gamma_j} (g_j\varphi - \nabla\varphi \,.\, \hat{n}\omega)\, \mathrm{d}s - \sum_j^D \int_{\Gamma_j} \nabla\varphi \,.\, \hat{n}f_j \, \mathrm{d}s + \int_\Omega p\varphi \, \mathrm{d}A \tag{7}$$

where $\sum_j^N$ and $\sum_j^D$ denote summation over all the edges Γ_j for which the Neumann boundary condition (3c) and the Dirichlet boundary condition (3b) apply, respectively. In general, some of the integrals in (7) will be singular. The expression (7) is in the form (1) with extraction functions $\zeta = \nabla^2\varphi$ and $\rho = -\nabla\varphi \cdot \hat{n}$, and load term

$$R = \sum_j^N \int_{\Gamma_j} g_j\varphi \, \mathrm{d}s - \sum_j^D \nabla\varphi \,.\, \hat{n}f_j \, \mathrm{d}s + \int_\Omega p\varphi \, \mathrm{d}A$$

Notice that if φ had the additional properties (i) $\nabla^2\varphi = 0$ in Ω, and (ii) $\nabla\varphi \,.\, \hat{n} = 0$ on the edges Γ_j for which the Neumann condition (3c) applies, then (7) would become simply

$$k_m = \sum_j^N \int_{\Gamma_j} g_j\varphi \, \mathrm{d}s - \sum_j^D \int_{\Gamma_j} \nabla\varphi \,.\, \hat{n}f_j \, \mathrm{d}s + \int_\Omega p\varphi \, \mathrm{d}A \tag{8}$$

The function φ could then be thought of as an influence function, relating the applied body force, boundary displacement and line loading to the resulting stress intensity factor k_m at O. In general, such a φ is not easily found.

In line with (2) we consider the approximation $\tilde{k}_m$ to k_m calculated using the finite element solution $\tilde{\omega}$,

$$\tilde{k}_m = \int_\Omega (\nabla^2\varphi)\tilde{v} \, \mathrm{d}A + \sum_j^N \int_{\Gamma_j} (g_j\varphi - \nabla\varphi \,.\, \hat{n}\tilde{\omega})\, \mathrm{d}s - \sum_j^D \int_{\Gamma_j} \nabla\varphi \,.\, \hat{n}f_j \, \mathrm{d}s + \int_\Omega p\varphi \, \mathrm{d}A \tag{9}$$

Much as in Reference 1, we shall see in Section 4 that the accuracy of $\tilde{k}_m$ is influenced by the smoothness of the extraction functions $\zeta = \nabla^2\varphi$ and $\rho = -\nabla\varphi \,.\, \hat{n}$. As before, the issue of how to select a φ for use in (9) is essentially a matter of deciding how to satisfy the boundary

requirement above in a smooth way. Among others, the cut-off function and blending function techniques described in Reference 1 may be used. We shall leave to Section 6 any further discussion of the actual numerical implementation of (9).

3 THE GENERALIZED ENERGY RELEASE METHOD

3.1 *Preliminaries*

The second approach that we shall discuss is related to the well-known energy release method of fracture mechanics. Over the years this method has been implemented in numerous forms. To name but a few: the J-integral,[6,9,10] the stiffness derivative[7] and the crack closure[8–10] methods. In common with these methods, the approach that we shall outline in this section only applies to cases where the included angle at the vertex O is π or 2π (i.e. $\alpha = 1, 2$). This restriction is not too serious since in practice these cases are by far the most important. Again, although we only discuss the model problem (3), the technique that we shall outline may be extended to treat other problems.

3.2 *Another expression for k_m*

Let φ be a smooth function on Ω (bounded first derivatives on Ω will suffice), and define

$$v = \frac{-4\alpha}{\pi(2m-1)(1-2\alpha-2m)} r^{(1+2\alpha-2m)(1/2\alpha)} \sin\left((1+2\alpha-2m)\frac{\theta}{2\alpha}\right) \qquad (m = 1, 2, \ldots) \tag{10}$$

For $\varepsilon > 0$, sufficiently small, and with Ω_ε, $\Gamma_j^{(\varepsilon)}$ and $\gamma_l^{(\varepsilon)}$ as in Subsection 2.2, define

$$\Phi_\varepsilon = \int_{\Omega_\varepsilon} (\nabla\omega)^{\mathrm{T}} \begin{pmatrix} -\varphi_{,1} & -\varphi_{,2} \\ -\varphi_{,2} & \varphi_{,1} \end{pmatrix} \nabla v \, dA$$

In fact,

$$\Phi_\varepsilon = \left(\sum_l \int_{\gamma^{(\varepsilon)}} + \sum_j \int_{\Gamma^{(\varepsilon)}}\right) \begin{pmatrix} \omega_{,1}v_{,1} + \omega_{,2}v_{,2} \\ -\omega_{,1}v_{,2} - \omega_{,2}v_{,1} \end{pmatrix} \cdot \hat{n}\varphi \, ds$$
$$- \int_{\Omega_\varepsilon} (-v_{,1}\nabla^2\omega - \omega_{,1}\nabla^2 v)\varphi \, dA \tag{11}$$

after an integration by parts. Here $\hat{n}$ denotes the outward pointing unit normal and $(\ )_{,i}$ indicates differentiation with respect to x_i.

Now, let us place some concrete restrictions on φ. Suppose that

1. $\varphi(O) = 1$, and
2. $\varphi = 0$ on $\Gamma_3, \Gamma_4, \ldots, \Gamma_s$ (i.e. on all Γ_j's except Γ_1 and Γ_2).

Now introducing the assumption $\alpha = 1, 2$, and noting that $v = 0$ on $\Gamma_1^{(\varepsilon)}$, $\nabla v \cdot \hat{n} = 0$ on $\Gamma_2^{(\varepsilon)}$ and $\nabla^2 v = 0$ in Ω_ε, then (11) becomes

$$\Phi_\varepsilon = \sum_l \int_{\gamma^{(\varepsilon)}} \begin{pmatrix} -\omega_{,1}v_{,1} + \omega_{,2}v_{,2} \\ -\omega_{,1}v_{,2} - \omega_{,2}v_{,1} \end{pmatrix} \cdot \hat{n}\varphi \, ds - \int_{\Omega_\varepsilon} v_{,1} p\varphi \, dA$$

Using (10) and the expansions (4), (5), we may evaluate the limiting values of these line integrals to find

$$\lim_{\varepsilon\to 0+}\left(\Phi_\varepsilon+\int_{\Omega_\varepsilon} v_{,1}\varphi p\,\mathrm{d}A\right)=k_m$$

If we assume

3. In the vicinity of the origin, $\nabla\varphi=O(r^\beta)$, where $\beta>\max(0,(m-\alpha-1)/\alpha)$,

then the integrand appearing in the definition of Φ_ε is integrable over Ω, and we have

$$k_m=\int_\Omega(\nabla\omega)^{\mathrm{T}}\begin{pmatrix}-\varphi_{,1} & -\varphi_{,2}\\ -\varphi_{,2} & \varphi_{,1}\end{pmatrix}\nabla v\,\mathrm{d}A+\lim_{\varepsilon\to 0+}\int_{\Omega_\varepsilon} v_{,1}p\varphi\,\mathrm{d}A \tag{12}$$

This is in the form required by (1), with extraction functions

$$\lambda_1=-\varphi_{,1}v_{,1}-\varphi_{,2}v_{,2}$$
$$\lambda_2=-\varphi_{,2}v_{,1}+\varphi_{,1}v_{,2}$$

$\zeta=0$, and $\rho=0$, and load term $R=\int v_{,1}p\varphi\,\mathrm{d}A$. The load term integral may be singular. Notice that requirement 2 applies independently of the nature of the boundary conditions on $\Gamma_3,\ldots,\Gamma_s$. This contrasts with the corresponding requirement 1 of Section 2 which only needs to hold on Γ_j's for which Dirichlet boundary conditions apply.

In accord with (2) we may use (8) with $\tilde{\omega}$ replacing ω to obtain an approximation $\tilde{k}_m$ to k_m. As usual, in practice we would want λ to be as smooth as possible. One strategy is to let φ be identically 1 in a neighbourhood of the origin and then let requirement 2 be imposed by smooth cut-off functions. The condition 3 is automatically satisfied. This strategy has the computational advantage of eliminating the need to evaluate an improper integral near the origin (since $\varphi_{,1}=\varphi_{,2}=0$ there).

It may not at first be apparent what connection the expression (12) has with the energy release principle. We shall not explain this in detail here (see Reference 13). However, let us just note two points. First, the matrix

$$\begin{pmatrix}-\varphi_{,1} & -\varphi_{,2}\\ -\varphi_{,2} & \varphi_{,1}\end{pmatrix}$$

can be thought of as a form of stiffness derivative with respect to crack extension, whereas secondly, the quantity

$$\begin{pmatrix}-\omega_{,1}v_1+\omega_{,2}v_{,2}\\ -\omega_{,1}v_{,2}-\omega_{,2}v_{,1}\end{pmatrix}.\hat{n}$$

which appears in the line integrals of (11) can, by formally putting $v=\omega$, be identified with

$$|\nabla\omega|^2 n_1-2\omega_{,1}\nabla\omega\,.\,\hat{n}.$$

Except for a factor of $\frac{1}{2}$, this is the term which appears in the J_1-integral associated with (3).

4 THE ACCURACY OF THE APPROXIMATIONS $\tilde{k}_m$

Our discussion in this section will be brief, since much of what we said in our earlier paper (see Subsection 3.4 of Reference 1) applies in the current setting also. Pursuing the same

argument as there leads, for the techniques of both Sections 2 and 3, to the error relation

$$k_m - \tilde{k}_m = \int_\Omega (\nabla(\omega - \tilde{\omega})) \,.\, \nabla(\psi - \tilde{\psi})\, dA \tag{13}$$

where ψ and $\tilde{\psi}$ are the exact and finite element solutions of the auxiliary problem,

$$\left.\begin{aligned} &-\nabla^2\psi = \nabla \,.\, \lambda + \zeta \quad \text{in } \Omega \\ &\psi = 0 \quad \text{on those } \Gamma_j \text{ for which the Dirichlet condition (3b) applies} \\ &\nabla\psi \,.\, \hat{n} = \lambda \,.\, \hat{n} + \rho \quad \text{on those } \Gamma_j \text{ for which the Neumann condition (3c) applies} \end{aligned}\right\} \tag{14}$$

using the notation of (1)/(2). (In obtaining (13) we have implicitly assumed that the Dirichlet data f_j is exactly representable by a finite element function. If this is not the case, then the expression (13) no longer applies. We shall not discuss this situation here.) This auxiliary problem is of the same form as the basic problem (3), with only the right-hand sides of the differential equation and boundary conditions changed. If we let $\mathscr{E}(.)$ denote the strain energy expression associated with the problem (3),

$$\mathscr{E}(.) = \int_\Omega |\nabla(.)|^2\, dA$$

then from (13) we obtain the usual estimate

$$\begin{aligned} |k_m - \tilde{k}_m| &\leq \mathscr{E}(\omega - \tilde{\omega})^{1/2} \mathscr{E}(\psi - \tilde{\psi})^{1/2} \\ &\leq \min_{\nu} \mathscr{E}(\omega - \nu)^{1/2} \min_{\nu^*} \mathscr{E}(\psi - \nu^*)^{1/2} \end{aligned} \tag{15}$$

where ν and ν^* range over all finite element functions which vanish on those Γ_j to which the Dirichlet condition (3b) applies.

The conclusion to be drawn from (15) is precisely the same as that which we have already noted in Reference 1: the accuracy of the post-processed value is related to how well the finite element functions are able to simultaneously approximate both the solution ω of the basic problem and the solution ψ of an auxiliary problem.

The corner points of Ω usually give rise to some form of singular behaviour in ω and ψ. This seriously affects how well these functions can be approximated by the finite element functions. None the less, it may be shown, in theory at least, that for suitable 'optimally refined' meshes, with pth degree elements $\min_\nu \mathscr{E}(\omega - \nu)^{1/2} = O(N^{-p/2})$, when N is the number of degrees-of-freedom of the finite element model. The same meshes also give $\min_{\nu^*} \mathscr{E}(\psi - \nu^*)^{1/2} = O(N^{-p/2})$, provided the right-hand sides in (14) are sufficiently smooth. For such meshes then, we have from (15), $|k_m - \tilde{k}_m| = O(N^{-p})$. Of course, from a practical point of view, the constant multiplying the N^{-p} in the $O(N^{-p})$ term is very important. The constant is related to, among other things, the smoothness of the right-hand sides of both the basic problem (3) and the auxiliary problem (13). *A priori*, little seems to be able to be said about choosing meshes that optimize its value. However, on a qualitative level, we again remark on the importance of choosing post-processing procedures with 'smooth' extraction functions λ, ε and ρ's.

Let us, however, remark on a point that we shall return to in greater detail in our next paper. Already, by concentrating our attention on the estimate (15) we have strayed somewhat from our real objective, which is to find high-accuracy approximations to k_m. The actual error

in $\tilde{k}_m$ is given by (13). The estimate (15) assumes the worst possible case, namely that there is no cancellation in the integral (13). If there is some cancellation, then $k_m - \tilde{k}_m$ will be overestimated by (15).

5 AN EXAMPLE FROM LINEAR ELASTICITY

Consider the edge-cracked square cylinder whose cross-section Ω is shown in Figure 3. We suppose that a plane strain assumption is valid. The crack faces Γ_1, Γ_2, Γ_3 and Γ_4 are traction free and the non-crack boundary of the region Ω has a traction loading of $g = (g_1, g_2)$. We assume that no body forces act. Let w denote the displacement vector and suppose that (r, θ) are polar co-ordinates centred at A.

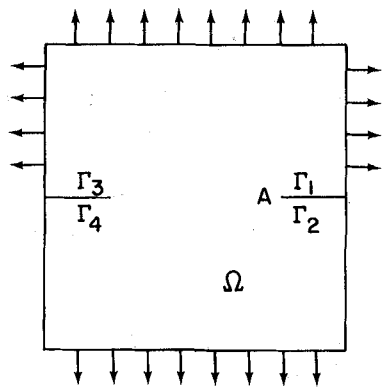

Figure 3. Cross-section of an edge-cracked square cylinder

In the neighbourhood of A the displacement vector w can be written in the form

$$w = \begin{pmatrix} w_1 \\ w_2 \end{pmatrix} \frac{K_I r^{1/2}}{2\mu} \begin{pmatrix} -\left(\kappa - \frac{1}{2}\right) \sin\frac{\theta}{2} - \frac{1}{2}\sin\frac{3\theta}{2} \\ \left(\kappa + \frac{1}{2}\right) \cos\frac{\theta}{2} + \frac{1}{2}\cos\frac{3\theta}{2} \end{pmatrix}$$

$$+ \frac{K_{II} r^{1/2}}{2\mu} \begin{pmatrix} -\left(\kappa + \frac{3}{2}\right) \cos\frac{\theta}{2} + \frac{1}{2}\cos\frac{3\theta}{2} \\ -\left(\kappa - \frac{3}{2}\right) \sin\frac{\theta}{2} + \frac{1}{2}\sin\frac{3\theta}{2} \end{pmatrix} + O(r^{3/2})$$

where μ is the shear modulus, $\kappa = 3\text{–}4\nu$ and ν is Poisson's ratio. The constants K_I and K_{II} are (up to a normalizing constant) the modes I and II stress intensity factors of linear fracture mechanics. There are a number of extraction expressions that yield the stress intensity factors K_I and K_{II}. We shall briefly describe two kinds of such expressions.

First, we consider an analogue of the generalized influence function method of Section 2. Define the vector functions ϕ^I and ϕ^{II} by

$$\phi^I = \begin{pmatrix} \phi_1^I \\ \phi_2^I \end{pmatrix} = \frac{r^{-1/2}}{2\mu} \begin{pmatrix} \left(-\kappa + \frac{3}{2}\right) \sin\frac{\theta}{2} - \frac{1}{2}\sin\frac{5\theta}{2} \\ -\left(\kappa + \frac{3}{2}\right) \cos\frac{\theta}{2} + \frac{1}{2}\cos\frac{5\theta}{2} \end{pmatrix}$$

and

$$\phi^{\mathrm{II}} = \begin{pmatrix} \phi_1^{\mathrm{II}} \\ \phi_2^{\mathrm{II}} \end{pmatrix} = \frac{r^{-1/2}}{2\mu} \begin{pmatrix} \left(\kappa + \frac{1}{2}\right)\cos\frac{\theta}{2} + \frac{1}{2}\cos\frac{5\theta}{2} \\ \left(-\kappa + \frac{1}{2}\right)\sin\frac{\theta}{2} + \frac{1}{2}\sin\frac{5\theta}{2} \end{pmatrix}$$

Then for $\alpha = \mathrm{I}, \mathrm{II}$ it may be shown that

$$K_\alpha = \frac{\mu}{4\pi(1-\nu)} \int_{\partial\Omega} (g_k \phi_k^\alpha - t_{kl}(\phi^\alpha) n_l w_k)\, \mathrm{d}s \tag{16}$$

where, for any vector functions u, $t_{kl}(u)$ denotes the corresponding stress tensor

$$t_{kl}(u) = \frac{2\mu\nu}{1-2\nu}\delta_{kl}\frac{\partial u_s}{\partial x_s} + \mu\left(\frac{\partial u_k}{\partial x_l} + \frac{\partial u_l}{\partial x_k}\right) \qquad (k, l, s = 1, 2)$$

$\hat{n} = (n_1, n_2)$ is the outward pointing unit normal on $\partial\Omega$; δ_{kl} is the Kronecker delta; and a repeated index indicates summation. Notice that the integration in (16) is, in fact, only over the non-crack portion of $\partial\Omega$.

The second kind of extraction expression that we shall describe is related to the generalized energy release method of Section 3. Suppose that ϕ is any sufficiently smooth function which is unity in the vicinity of A and vanishes on $\partial\Omega - (\Gamma_1 \cup \Gamma_2)$. Let

$$v^{\mathrm{I}} = \begin{pmatrix} v_1^{\mathrm{I}} \\ v_2^{\mathrm{I}} \end{pmatrix} = \frac{r^{1/2}}{2\mu} \begin{pmatrix} -\left(\kappa - \frac{1}{2}\right)\sin\frac{\theta}{2} - \frac{1}{2}\sin\frac{3\theta}{2} \\ \left(\kappa + \frac{1}{2}\right)\cos\frac{\theta}{2} + \frac{1}{2}\cos\frac{3\theta}{2} \end{pmatrix}$$

and

$$v^{\mathrm{II}} = \begin{pmatrix} v_1^{\mathrm{II}} \\ v_2^{\mathrm{II}} \end{pmatrix} = \frac{r^{1/2}}{2\mu} \begin{pmatrix} -\left(\kappa + \frac{3}{2}\right)\cos\frac{\theta}{2} + \frac{1}{2}\cos\frac{3\theta}{2} \\ -\left(\kappa - \frac{3}{2}\right)\cos\frac{\theta}{2} + \frac{1}{2}\sin\frac{3\theta}{2} \end{pmatrix}$$

Then for $\alpha = \mathrm{I}, \mathrm{II}$

$$K_\alpha = \frac{-\mu}{(1-\nu)\pi} \int_\Omega \left\{ \left(\frac{\partial w_i}{\partial x_k} t_{ik}(v^\alpha) - \frac{\partial w_i}{\partial x_1} t_{i1}(v^\alpha) - \frac{\partial v_i}{\partial x_1} t_{i1}(w) \right) \frac{\partial \phi}{\partial x_1} \right.$$
$$\left. - \left(\frac{\partial w_i}{\partial x_1} t_{i2}(v^\alpha) + \frac{\partial v_i^\alpha}{\partial x_1} t_{i2}(w) \right) \frac{\partial \phi}{\partial x_2} \right\} \mathrm{d}A \tag{17}$$

Notice that the integration in (17) excludes the region around A in which $\phi = 1$. Therefore, the singularities in the derivatives of v^α at A should present no computational difficulties in any post-processing based on (17).

6 SOME NUMERICAL EXAMPLES

6.1 *The FEARS program*

The calculations associated with the examples of this section were performed using the FEARS program. FEARS is a research oriented, adaptive finite element package developed

at the University of Maryland. A detailed description of the operation of the program can be found in Reference 11. For the purposes of this paper, the following few remarks will suffice. FEARS assumes that the region under consideration has, first, been partitioned into a number of subregions, each of which is a curvilinear quadrilateral. Within the program, each of these subregions is transformed by a change of co-ordinates into a unit square. The actual finite element modelling is then carried out on these transformed squares. Square bilinear elements are used. FEARS has an adaptive character: starting from an initial coarse mesh (usually, uniform on each of the transformed squares), the program automatically selects, in a recursive manner, a sequence of 'optimal' mesh refinements. FEARS also calculates an *a posteriori* estimate of the error in the finite element solution. The automatic mesh refinement process is based upon this error estimate.

6.2 *Example A: a slit, circular membrane*

Let Ω be the unit circle slit along the positive X_1 axis. In the notation of Subsection 1.2 let Γ_1 be the upper face of the slit, Γ_2 the lower face of the slit and Γ_3 the circular portion of the boundary of Ω. We consider the following particular case of the model problem (3):

$$\begin{aligned} \nabla^2\omega &= 0 \quad \text{in } \Omega \\ \omega &= 0 \quad \text{on } \Gamma_1 \\ \frac{\partial\omega}{\partial n} &= 0 \quad \text{on } \Gamma_2 \\ \frac{\partial\omega}{\partial n} &= x_2 \quad \text{on } \Gamma_3 \end{aligned} \tag{18}$$

(See Figure 4.) For this problem the expansion (4) about the origin takes the form

$$\begin{aligned} \omega &= k_1 r^{1/4}\sin\frac{\theta}{4} + k_2 r^{3/4}\sin\frac{3\theta}{4} + k_3 r^{5/4}\sin\frac{5\theta}{4} + O(r^{7/4}) \\ \nabla\omega &= \frac{k_1 r^{-3/4}}{4}\begin{pmatrix}\sin(-\frac{3}{4}\theta)\\ \cos(-\frac{3}{4}\theta)\end{pmatrix} + \frac{3k_2 r^{-1/4}}{4}\begin{pmatrix}\sin(-\frac{1}{4}\theta)\\ \cos(-\frac{1}{4}\theta)\end{pmatrix} \\ &\quad + \frac{5k_3 r^{1/4}}{4}\begin{pmatrix}\sin\frac{\theta}{4}\\ \cos\frac{\theta}{4}\end{pmatrix} + O(r^{3/4}) \end{aligned} \tag{19}$$

Using the method of separation of variables, an infinite series representation of ω may be found. This series can be manipulated to give the following exact values (correct to six significant figures):

$$\mathscr{E}(\omega) = \int_\Omega |\nabla\omega|^2 \, dA = 4{\cdot}52707$$

$$k_1 = -1{\cdot}35812 \qquad k_2 = 0{\cdot}970087 \qquad k_3 = 0{\cdot}452707$$

(Note that the influence functions for the k_m are actually readily available in the present case. They are given by

$$\varphi = \frac{2}{\pi(2m-1)}\left(r^{-(2m-1)(1/2\alpha)} + r^{(2m-1)(1/2\alpha)}\right)\sin\left((2m-1)\frac{\theta}{2\alpha}\right.$$

as may be easily verified. The k_m are given by (8).)

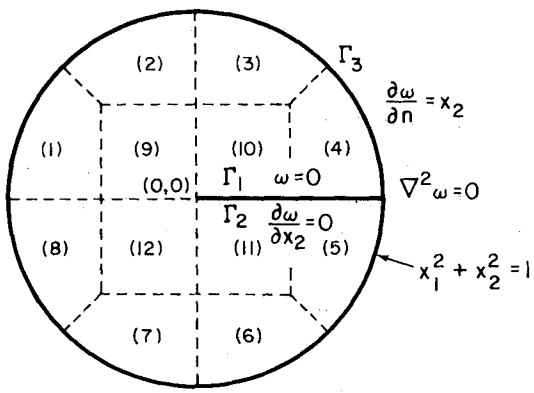

Figure 4. The region for Example A

Table I lists some properties of a sequence of five adaptively refined meshes produced by the FEARS program for the problem (18) with Ω partitioned as in Figure 4. FEARS was directed in this instance to produce refinements that were 'optimal' in the strain energy sense. Mesh I is uniform on each of the transformed squares. Subsequent meshes exhibit, as would be expected, quite severe refinement about the tip of the slit. (Figure 5 shows the mesh on subregions 9, 10, 11 and 12 in the case of mesh IV.) Using the approximate solutions corresponding to each of these meshes, we calculated two sets of approximations $\tilde{k}_1$, $\tilde{k}_2$ and $\tilde{k}_3$ to the first three stress intensity factors of (19). First, we used the generalized influence function method of Section 2, obtained by choosing

$$\varphi = \frac{2}{(\pi(2m-1)}r^{-(2m-1)\frac{1}{4}}\sin\left((2m-1)\frac{\theta}{4}\right)$$

in (7). This gives the expression

$$\tilde{k}_m = \int_{\Gamma_3}(x_2\varphi - \nabla\varphi \,.\, \hat{n}\tilde{\omega})\,ds \tag{20}$$

Notice that for this example the requirement 1 of Section 2 does not apply to Γ_3. There is no need for us to make φ vanish there. Secondly, we used the generalized energy release method of Section 3 with

$$\rho(x_1, x_2) = \begin{cases} 1 & 0 \leq r < \frac{1}{2} \\ 1 - 4(r-\frac{1}{2})^2 & \frac{1}{2} \leq r \leq 1 \end{cases}$$

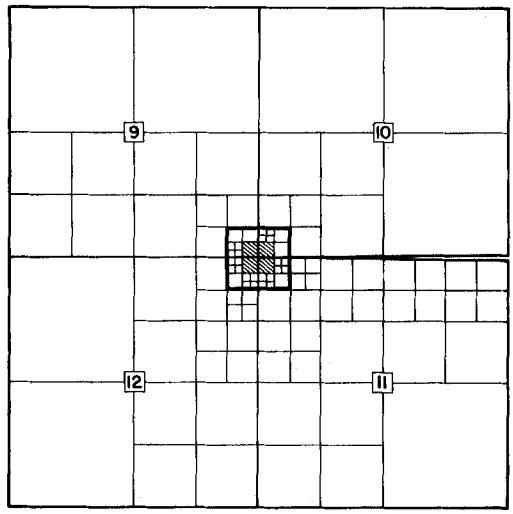

(i) Mesh on subregions 9, 10, 11 and 12

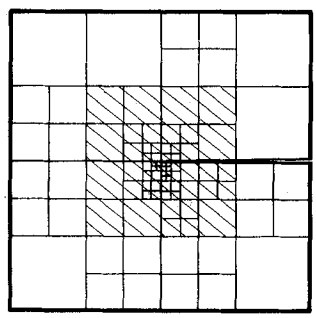

(ii) Details of mesh in shaded region of (i)

Figure 5. Mesh IV of Example A

Table I. Table of properties of an adaptive sequence of meshes for Example A

Mesh label	I	II	III	IV	V
Number of degrees-of-freedom	56 (uniform mesh)	89	118	171	391
Energy $\mathscr{E}(\tilde{\omega})$ (exact energy = 4·52707)	4·09456	4·26127	4·37694	4·45831	4·50090
Relative energy norm of error $=\left(\frac{\mathscr{E}(\omega-\tilde{\omega})}{\mathscr{E}(\omega)}\right)^{1/2}$	30·9%	24·2%	18·2%	12·3%	7·6%

in (12). This gives the expression

$$\tilde{k}_m = \int_{|r|=\frac{1}{2}} \nabla\tilde{\omega} \begin{pmatrix} -\cos\theta & -\sin\theta \\ -\sin\theta & \cos\theta \end{pmatrix} \nabla v(-8(r-\tfrac{1}{2}))\, dA \tag{21}$$

with v given by (10) with $\alpha = 2$. The results of these computations are displayed in Table II.

Table II. Table of computed values of $\tilde{k}_m$ $(m = 1, 2, 3)$ for Example A

Mesh label	Generalized influence function method (% relative error)			Generalized energy release method (% relative error)		
	$\tilde{k}_1$	$\tilde{k}_2$	$\tilde{k}_3$	$\tilde{k}_1$	$\tilde{k}_2$	$\tilde{k}_3$
I	−1·164426 (14·3%)	0·967356 (0·28%)	0·451378 (0·29%)	−1·17254 (13·7%)	0·968795 (0·13%)	0·450182 (0·56%)
II	−1·23455 (0·1%)	0·970937 (0·09%)	0·451417 (0·29%)	−1·24476 (8·3%)	0·973122 (0·31%)	0·449987 (0·60%)
III	−1·29103 (4·9%)	0·969749 (0·03%)	0·451598 (0·25%)	−1·30099 (4·2%)	0·971952 (0·19%)	0·450167 (0·56%)
IV	−1·32898 (2·1%)	0·969526 (0·06%)	0·451743 (0·21%)	−1·33666 (1·6%)	0·971219 (0·12%)	0·450974 (0·38%)
V	−1·34743 (0·79%)	0·969756 (0·03%)	0·452307 (0·09%)	−1·35188 (0·46%)	·0·970560 (0·05%)	0·452109 (0·13%)
Exact value	−1·35812	0·970087	0·452707	−1·35812	0·970087	0·452707

The following conclusions may be drawn from the results shown in Tables I and II:

1. Despite the presence of an $r^{1/4}$-type singularity at the slit tip, the sequence of adaptively created meshes gives an apparent rate of convergence for the energy norm of the error that is at least as good as the theoretically 'optimal refinement' rate of $O(N^{-1/2})$, where N is the number of degrees-of-freedom of the finite element model. The refinement step from Mesh IV to Mesh V has an apparent convergence rate of $O(N^{-0.6})$. The earlier steps show an even faster rate. Had only uniform meshes been used on the transformed squares, theory would have predicted an $O(N^{-0.125})$ rate. In that case, to obtain an accuracy in the energy norm comparable to that of the present mesh V, approximately 4×10^6 degrees-of-freedom would have been required. This would clearly not be a practical proposition.
2. There seems to be no significant difference between the $\tilde{k}_m$'s calculated using the influence function method and those calculated by the energy release method. Observe that in both cases $\tilde{k}_1$ appears to be converging at a rate twice that of the energy norm of the error. The IV to V refinement step shows an apparent rate of convergence of about $O(N^{-1.2})$ and $O(N^{-1.4})$ for the influence function and energy release methods, respectively. This is consistent with the theory we briefly discussed in Section 4. We saw there, that the error in $\tilde{k}_m$ could be expected to be of the order of the square of the energy norm of the error in $\tilde{\omega}$. For 'optimally refined'

meshes this would give

$$|k_m - \tilde{k}_m| = O(N^{-1}).$$

3. The coefficients $\tilde{k}_2$ and $\tilde{k}_3$ are markedly more accurate than $\tilde{k}_1$. Even for the coarsest mesh considered, they have relative errors of around 0·5 per cent. This is attributable to the relative smoothness of the solution ψ of the auxiliary problem (14) in each of these cases. The values of $\tilde{k}_2$ and $\tilde{k}_3$ appear to behave erratically as the meshes are refined. Quadrature errors made in numerically evaluating (20) and (21) are responsible for this.

We shall now utilize these post-processed values $\tilde{k}_1$, $\tilde{k}_2$ and $\tilde{k}_3$ in the expansions given in (19) to obtain approximations for ω and $\nabla\omega$ at points near (0, 0). Some typical numerical results for ω and $\partial\omega/\partial x_1$ at points along Γ_2 are recorded in Table III. The values of $\tilde{k}_m$ used were those calculated by the generalized influence function method. By virtue of our comment in paragraph 1 above, use of the $\tilde{k}_m$'s computed by (21) would not have significantly altered our results. In Table III we have also indicated the exact values (to six significant figures) for the quantities of interest. The standard finite element technique for finding pointwise approximations to ω or $\partial\omega/\partial x_1$ would be to simply evaluate the finite element solution $\tilde{\omega}$ or its derivative $\partial\tilde{\omega}/\partial x_1$ at the relevant point. For comparison, we have listed the results of this standard approach in parentheses under the entries of Table III.

The accuracy of the post-processing approximations for ω and $\partial\omega/\partial x_1$ will be affected by both the accuracy of the $\tilde{k}_m$'s used and the truncation error made by only considering the first three terms of the expansion (19). The latter effect will become less significant as $r \to 0$, while for a fixed r it can, of course, be diminished by taking a larger number of terms in the expansion (19). Finally, let us just say a few words about the particular results shown in Table III. Even for the coarsest mesh I (it is uniform on the transformed squares) with $r \sim 0{\cdot}1$, the post-processed

Table III. Results of post-processing calculations for ω and $\partial\omega/\partial x_1$ for Example A (the quantities in parentheses are the approximations obtained using the standard method)

Mesh label	$\omega(r, 2\pi)$			$\frac{\partial\omega}{\partial x_1}(r, 2\pi)$	
	$r = 1/8$	$r = (1/8)^2$	$r = (1/8)^3$	$r = 0{\cdot}1$	$r = 0{\cdot}1$
I	−0·862086 (−0·413282)	−0·451886 (−0·051660)	−0·253558 (−0·006458)	−2·60967 (−3·30626)	−11·3201 (−3·30626)
II	−0·904630 (−0·708604)	−0·476895 (−0·088576)	−0·268367 (−0·011072)	−2·71323 (−3·08754)	−11·8843 (−8·25013)
III	−0·937950 (−0·825429)	−0·496811 (−0·345869)	−0·280230 (−0·043234)	−2·79092 (−2·70173)	−12·3279 (−22·1356)
IV	−0·960458 (−0·908886)	−0·510217 (−0·443701)	−0.288206 (−0·195142)	−2·84388 (−2·62627)	−12·6274 (13·1755)
V	−0·971435 (−0·952252)	−0·516747 (−0·492745)	−0·292086 (−0·257192)	−2·86972 (−2·71021)	−12·7736 (−13·9043)
Exact value	−0·975118	−0·520476	−0·294335	−2·85196	−12·8536

values for both ω and $\partial\omega/\partial x_1$ are all within around 10 per cent of the exact values. Quite generally throughout the table, the post-processed values have about one extra decimal place of accuracy than the corresponding standard approximation.

6.3 *Example B: a semicircular membrane with a free half-edge*

This time let Ω be the semicircular region depicted in Figure 6. We shall consider the following particular case of the model problem (3):

$$\begin{aligned} \nabla^2\omega &= -1 \quad \text{in } \Omega \\ \omega &= 0 \quad \text{on } \Gamma_1 \text{ and } \Gamma_3 \\ \frac{\partial\omega}{\partial n} &= 0 \quad \text{on } \Gamma_2 \end{aligned} \tag{22}$$

For this problem the expansion (4) is valid with $\alpha = 1$ and $N = 2$,

$$\omega = k_1 r^{1/2} \sin\frac{\theta}{2} + k_2 r^{3/2} \sin\frac{3\theta}{2} + O(r^2)$$

$$\nabla\omega = \frac{k_1 r^{-1/2}}{2}\begin{pmatrix} \sin\left(-\frac{\theta}{2}\right) \\ \cos\left(-\frac{\theta}{2}\right) \end{pmatrix} + \frac{3k_2 r^{1/2}}{2}\begin{pmatrix} \sin\frac{\theta}{2} \\ \cos\frac{\theta}{2} \end{pmatrix} + O(r)$$

As for Example A, an infinite series representation for ω can be found. This permits the calculation of the following exact values (correct to six significant figures):

$$E(\omega) = \int_\Omega |\nabla\omega|^2 \, dA = 0{\cdot}109757$$

$$k_1 = 0{\cdot}339531 \qquad k_2 = 0{\cdot}242522$$

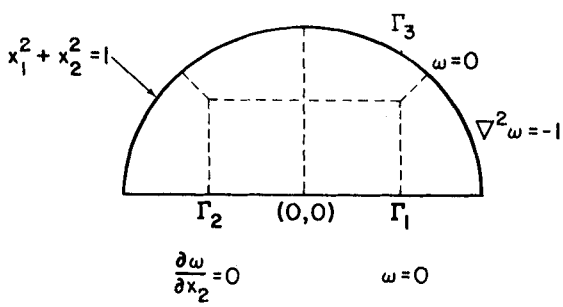

Figure 6. The region for Example B

Table IV lists some features of a sequence of five adaptively refined meshes which were created by FEARS for this problem. The initial partitioning of Ω into subregions is shown in Figure 6. As in Example A, FEARS was directed to produce refinements that were 'optimal' in the strain energy sense. Again the initial mesh I was chosen to be uniform on each of the transformed squares, and the subsequent automatically created meshes show the expected refinement around the critical point (0, 0).

Table IV. Table of properties of an adaptive sequence of meshes for Example B

Mesh label	I	II	III	IV	V
Number of degrees-of-freedom	20 (uniform mesh)	40	91	126	534
Energy $\mathscr{E}(\tilde{\omega})$ (exact energy = 0·109757)	0·100361	0·104180	0·107401	0·108326	0·109362
Relative energy norm of error $=\left(\frac{\mathscr{E}(\omega-\tilde{\omega})}{\mathscr{E}(\omega)}\right)^{1/2}$	29·3%	22·5%	14·7%	11·4%	6·0%

Using the finite element solutions for each of these meshes, two sets of post-processed approximations to the stress intensity factors k_1 and k_2 of (22) were computed. First, the generalized influence function method of Section 2 was employed with

$$\phi = X(x)\frac{2}{\pi(2m-1)}r^{-(2m-1)\frac{1}{2}}\sin\left((2m-1)\frac{\theta}{2}\right) \qquad (m=1,2)$$

where

$$X(x)=\begin{cases}1 & \text{if } 0\leqslant r<\frac{1}{2}\\ 1-8(r-\frac{1}{2})^3 & \text{if } \frac{1}{2}\leqslant r\leqslant 1\end{cases} \qquad (23)$$

The function X is a radially symmetric cut-off function. In contrast to the case of Example A, we here have to require that $\varphi=0$ on Γ_3 since the original problem (22) has a Dirichlet boundary condition there. The expression (9) now specializes to

$$\tilde{k}_m=\int_\Omega \nabla^2\varphi\tilde{\omega}\,\mathrm{d}A+\int_\Omega \varphi\,\mathrm{d}A$$

where the last integral is singular. It may of course be evaluated analytically, although it can be transformed so as to allow a numerical quadrature. To see how, let $z=\frac{1}{2}x_2^2$ and $\Omega_{(\varepsilon)}=\{x\in\Omega, r>\varepsilon\}$. Observe that integrating by parts and using the boundary conditions on φ leads to

$$\begin{aligned}\int_{\Omega_{(\varepsilon)}}\varphi\,\mathrm{d}A&=\int_{\Omega_{(\varepsilon)}}\varphi\nabla^2 z\,\mathrm{d}A=\int_{\partial\Omega_{(\varepsilon)}}(\varphi\nabla z\,.\,\hat{n}-\nabla\varphi\,.\,\hat{n}z)\,\mathrm{d}s+\int_{\Omega_{(\varepsilon)}}\nabla^2\varphi z\,\mathrm{d}A\\&=\left(\int_{\Gamma_3}+\int_{r=\varepsilon(0<\theta<\pi)}\right)(\varphi\nabla z\,.\,\hat{n}-\nabla\varphi\hat{n}z)\,\mathrm{d}s+\int_{\Omega_{(\varepsilon)}}\nabla^2\varphi z\,\mathrm{d}A\\&=\int_{\Gamma_3}(\varphi\nabla z\,.\,\hat{n}-\nabla\varphi\,.\,\hat{n}z)\,\mathrm{d}s+O(\varepsilon^{5/2-m})+\int_{\Omega_{(\varepsilon)}}\nabla^2\varphi z\,\mathrm{d}A\end{aligned}$$

Therefore,

$$\lim_{\varepsilon\to 0}\int_{\Omega_{(\varepsilon)}}\varphi\,\mathrm{d}A=\int_{\Gamma_2}(\varphi\nabla z\,.\,\hat{n}-\nabla\varphi\,.\,\hat{n}z)\,\mathrm{d}s+\int_\Omega\nabla^2\varphi z\,dA$$

and both these integrals are proper.

The second set of approximations is basedon the generalized energy release method of Section 3. Here, we choose for the functions φ and v of (12),

$$\varphi(x) = \begin{matrix} 1 & 0 \leqslant r < \frac{1}{2} \\ 1-4(r-\frac{1}{2})^2 & \frac{1}{2} \leqslant r \leqslant 1 \end{matrix}$$

and v as given by (10) with $\alpha = 1$ and $m = 1, 2$. The extraction expression (12) takes the specific form

$$\tilde{k}_m = \int_{r \geqslant 1/2} (\nabla \tilde{\omega})^{\mathrm{T}} \begin{pmatrix} -\cos\theta & -\sin\theta \\ -\sin\theta & \cos\theta \end{pmatrix} \nabla v(-8(r-\tfrac{1}{2}))\, \mathrm{d}A + \int_{\Omega} v_{,1}\varphi\, \mathrm{d}A$$

The second integral is singular. It may be evaluated analytically; however, it also can be expressed in a form which permits an effective numerical integration. An integration by parts gives

$$\begin{aligned} \int_{\Omega(\varepsilon)} v_{,1}\varphi\, \mathrm{d}A &= \int_{\partial\Omega_{(\varepsilon)}} v\varphi n_1\, \mathrm{d}s - \int_{\Omega_{(\varepsilon)}} v\varphi_{,1}\, \mathrm{d}A \\ &= O(\varepsilon^{5/2-m}) - \int_{\Omega_{(\varepsilon)}} v\varphi_{,1}\, \mathrm{d}A \end{aligned}$$

by virtue of the boundary conditions on φ. Since φ is identically 1 in a neighbourhood of the origin, this last integral is proper. Thus for $m = 1, 2$

$$\lim_{\varepsilon \to 0+} \int_{\Omega_{(\varepsilon)}} v_{,1}\varphi\, \mathrm{d}A = -\int_{\Omega} v\varphi_{,1}\, \mathrm{d}A$$

and this integral presents no quadrature difficulties.

The results of both the above sets of approximations are displayed in Table V. Tables IV and V present a picture very similar to that of the corresponding Tables I and II of Example A. Again we see an apparent rate of convergence for the energy norm of the error that is close to the 'optimal refinement' rate of $N^{-1/2}$, where N is the number of degrees-of-freedom of the finite element model. (The III to V refinement step behaves as $N^{-0.51}$, the IV to V step as $N^{-0.44}$). For this problem there is an $r^{1/2}$-type singularity near (0, 0). If only uniform meshes had been used, then theory would predict an $O(N^{-1/4})$ rate. To achieve an accuracy comparable to our adaptive mesh IV, about 900 degrees-of-freedom would be required. This is around seven times the number for mesh IV.

The values of $\tilde{k}_2$ are markedly more accurate than the corresponding approximations $\tilde{k}_1$. Again this can be related to the relative smoothness of the auxiliary functions of Section 4 in cases where $m = 2$. The apparent rates of convergence of $\tilde{k}_1$ for both the generalized influence function and generalized energy release methods are close to the 'optimal refinement' rate of $O(N^{-1})$. (The IV to V refinement step shows $N^{-0.92}$ and $N^{-0.90}$ rates for the two methods, respectively.) The two methods again yield accuracies that are much the same. The slightly poorer accuracy of the generalized influence function method can probably be traced to the sharp fall-off in the cut-off function X (see (23)) near Γ_3 and the consequences this has for the smoothness of associated auxiliary function of Section 4.

6.4 *Conclusions*

For these examples we see that the use of post-processing techniques allied with an appropriate adaptive mesh selection algorithm, makes it possible to obtain the leading stress intensity factor with say a 5 per cent accuracy, while using only a moderate number of degrees-of-freedom in

Table V. Table of computed values of $\tilde{k}_m$ $(m = 1, 2)$ for Example B

Mesh label	Generalized influence function method (% relative error)		Generalized energy release method (% relative error)	
	$\tilde{k}_1$	$\tilde{k}_2$	$\tilde{k}_1$	$\tilde{k}_2$
I	0·365049 (7·5%)	0·243906 (0·57%)	0·358583 (5·6%)	0·243055 (0·22%)
II	0·358329 (5·5%)	0·243806 (0·53%)	0·353765 (4·2%)	0·243438 (0·38%)
III	0·34824 (2·6%)	0·242934 (0·17%)	0·345217 (1·7%)	0·242769 (0·10%)
IV	0·344323 (1·4%)	0·242854 (0·14%)	0·342874 (0·98%)	0·242672 (0·06%)
V	0·340801 (0·37%)	0·242604 (0·03%)	0·340455 (0·27%)	0·242563 (0·02%)
Exact value	0·339531	0·242522	0·339531	0·242522

the finite element model (around 120 for our Example A). This, even though the strain energy norm of the error for such a mesh may still be of the order of 20 per cent (as in Example A). This latter observation highlights the importance of being specific when speaking of the accuracy of a finite element solution—a solution giving acceptable accuracy in one measure, may not be acceptable in another.

REFERENCES

1. I. Babuška and A. Miller, 'The post-processing approach in the finite element method—part 1: calculation of displacements, stresses and other higher derivatives of the displacements', *Int. j. numer. methods eng.*, **20**, 1085–1109 (1984).
2. P. Grisvard, 'Boundary value problems in non-smooth domains', *Lecture Notes No. 19*, Univ. of Maryland, Dept. of Mathematics (1980).
3. M. Š. Birman and G. E. Skvorcov, 'On the square integrability of the highest derivatives of the solution of the Dirichlet problem on domains with piecewise smooth boundaries' (in Russian), *Izvestija Vyšich Učebnych Zavedenij*, Math. 1962, no. 5, pp. 12–21.
4. M. Dobrowolski, *Numerical Approximation of Elliptic Interface and Corner Problems*, Habilitationsschrift, University of Bonn, 1981.
5. H. Blum, 'A simple and accurate method for the determination of stress intensity factors and solutions for problems on domains with corners', in *The Mathematics of Finite Elements and Applications IV*, MAFELAP, 1981 (Ed. J. R. Whiteman), Academic Press, London, 1982.
6. J. R. Rice, 'Mathematical analysis in the mechanics of fracture', in *Fracture: An Advanced Treatise*, vol. II (Ed. H. Liebowitz), Academic Press, New York, 1968, pp. 191–311.
7. D. M. Parks, 'A stiffness derivative finite element technique for determination of crack tip stress intensiy factors', *Int. J. Fract.*, **10**(4), 487–502 (1974).
8. T. K. Helen, 'On the method of virtual crack extensions', *Int. j. numer. methods eng.*, **9**(1), 187–207 (1975).
9. E. M. Morozov and G. P. Nikiškov, The Finite Element Method in Fracture Mechanics (in Russian), Nauka, Moscow, 1980.
10. *Computational Fracture Mechanics*, Proceedings of ASME 2nd National Congress on Pressure Vessels and Piping, San Francisco, June 1975 (Eds. E. F. Rybicki and S. E. Benzley), A.S.M.E., New York, 1975.
11. C. Mesztenyi and W. Szymczak, 'FEARS user's manual', *Technical Note No. BN-991*, Inst. for Physical Science and Technology, Univ. of Maryland (1982).
12. H. F. Bueckner, 'Field singularities and related integral representations', in *Mechanics of Fracture I*, 'Methods of Analysis and Solutions of Crack Problems' (Ed. G. C. Sih), Noordhoff, Leyden, 1973.
13. A. Miller, *The Calculation of Stress Intensity Factors* (in preparation).